Proceedings of ICRC 2001: 1025 © Copernicus Gesellschaft 2001

ICRC 2001

Atmospheric muon fluxes underwater as a tool to probe the small-x gluon distribution

A. Misaki[1], **T. S. Sinegovskaya**[2], **S. I. Sinegovsky**[2], **and N. Takahashi**[3]

[1]Waseda University, Ookubo 3-4-1, Shinjyuku-ku, Tokyo, 169-8555 Japan
[2]Irkutsk State University, Irkutsk, 664003 Russia
[3]Hirosaki University, Hirosaki, 036-8561 Japan

Abstract. We compute deep-sea energy spectra and zenith-angle distributions of the atmospheric muons, both conventional and prompt. The prompt muon contribution to the muon flux underwater is calculated taking into consideration predictions of recent charm production models in which probed is the small-x behavior of the gluon distribution inside of a nucleon. We argue for a possibility to discriminate the PQCD models of the charm production differing in the slope of the gluon distribution, in measurements with neutrino telescopes of the muon flux at energies 10-100 TeV.

1 Introduction

A correct treatment of the charm hadroproduction is important to the atmospheric muon and neutrino studies since short-lived charmed particles, $D^{\pm}$, D^0, $\overline{D}^0$, $D_s^{\pm}$, Λ_c^+, produced in collisions of cosmic rays with nuclei of the air, become the dominant source of atmospheric muons and neutrinos at energies $E \sim 100$ TeV. Thus, one needs to take them into consideration as the background for extraterrestrial neutrinos (Learned and Mannheim, 2000). Muons originating from decay of these charmed hadrons are so called prompt muons (PM) that contribute to the total atmospheric muon flux.

Another aspect of the interest to the charm production relates to the gluon density at small gluon momentum fraction x. The gluon density at small x is of considerable importance because this influences strongly the charm production cross section, both total and inclusive. Recently Pasquali et al. (1999) and Gelmini et al. (2000, 2001) have analyzed the influence of small-x behavior of the parton distribution functions (PDFs) to the atmospheric lepton fluxes at the sea level. Basing on next-to-leading order (NLO) calculations of the perturbative Quantum Chromodynamics (PQCD), they predict PM fluxes at the sea level depending strongly on proton gluon distributions at small x scale, $x < 10^{-5}$.

Correspondence to: S. I. Sinegovsky
(inegovsky@api.isu.runnet.ru)

The muon spectra underwater computed with the model of Pasquali et al. (1999), in which used were the MRSD_ (Martin et al., 1993) and the CTEQ3M (Lai et al., 1995) sets of PDFs, were recently discussed (Naumov et al., 2000; Sinegovskaya and Sinegovsky, 2001). In this talk, using predictions of more recent PQCD model (Gelmini et al., 2000, 2001) of the charm production, we discuss the PM contribution to muons underwater at depths typical for operating and constructing neutrino telescopes (AMANDA Collab., 2000; ANTARES Collab., 2000; Baikal Collab., 1997; NESTOR Collab., 2000). Namely, we try to study a PM flux underwater dependence on the slope λ of the gluon PDF at small x: $xg(x) \propto x^{-\lambda}$. The nature of the small-x behavior of the gluon density is now under extensive discussion (see, for example, Ball and Landshoff (2000); Schleper (2001); Vogt (2000); Yoshida (2001)). The small-x behavior of the PDFs is the subject of the deep interest since the realization of the underlying dynamics is yet far from being complete.

2 PDFs and charm production models

Due to dominant subprocess in heavy quarks hadroproduction, $gg \to c\bar{c}$, the charm production is sensitive to the gluon density at small x, where x is the gluon momentum fraction. One may evaluate the scale of x in cosmic ray interactions as follows. The product of the gluon momentum fraction x_1 of the projectile nucleon and that of the target x near the charm production threshold ($\sim 2m_c$) is $x_1 x = 4m_c^2/(2m_N E_0)$, where E_0 is the primary nucleon energy in the lab frame. Since a muon takes away about 5% of the primary nucleon energy, $E_0 \simeq 20E_\mu$, we have $x_1 x = 0.1(m_c/m_N)(m_c/E_\mu)$. Because of the steepness of the primary cosmic ray spectrum only large x_1 contribute sizeably to the atmospheric charm production, one needs adopt $x_1 \gtrsim 0.1$. Taking $m_c^2 \simeq 2$ GeV^2, one may find for $E_\mu \gtrsim 100$ TeV the range of importance to be $x \lesssim 2 \cdot 10^{-6}$. It should be stressed, this range is yet outside of the scope of the perturbative next-to-leading order global analysis of parton distributions (Martin et al.,

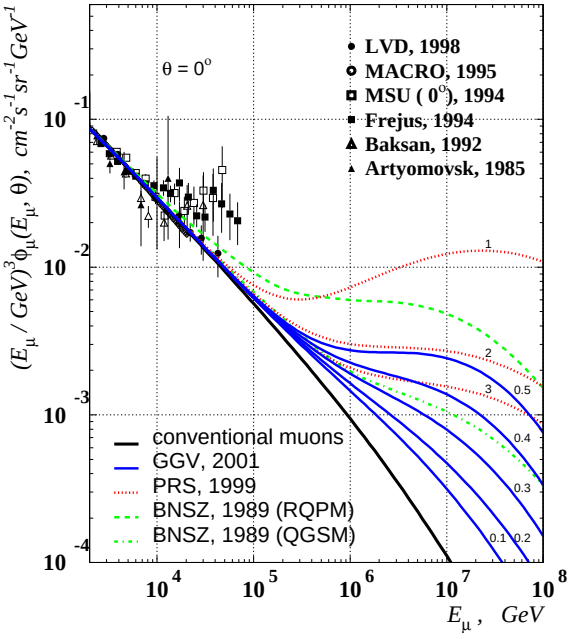

Fig. 1. Vertical sea-level muon flux predictions. (See Bugaev et al. (1998); Sinegovskaya and Sinegovsky (2001) for data references.)

1999; Lai et al., 2000).

The spectral index λ being used in the PQCD charm production models (Pasquali et al., 1999; Gelmini et al., 2001) covers wide range from about 0.1, the number that may be connected to the soft pomeron with intercept $1+\epsilon_0$ (where $\epsilon_0 = 0.08$), to about 0.5 in the 3-flavor scheme of the BFKL approach (Balitsky et al., 1978).

In Fig. 1 shown are sea-level PM fluxes (added to the conventional muon flux) predicted with PQCD charm production models by Pasquali et al. (1999) (hereafter PRS) and by Gelmini et al. (2000, 2001) (GGV), which are used in our calculation of the deep-sea muon flux. Let us sketch out these models.

PRS-1:

The PRS-1 model (dot lines in Figs. 1, 2) (identical with the PQCD-1 in Ref. (Sinegovskaya and Sinegovsky, 2001)) is based on the MRSD$_-$ set (Martin et al., 1993). The PDF input parameters are the followings: $xg(x,Q_0^2) \sim x^{-0.5}$ as $x \to 0$, 4-momentum transfer squared $Q_0^2 = 4\,\mathrm{GeV}^2$; the sea light quark asymmetry, $\overline{u} < \overline{d}$, is taking into consideration; the QCD scale in the minimal subtraction scheme ($\overline{\mathrm{MS}}$), $\Lambda_4^{\overline{\mathrm{MS}}} = 0.215\,\mathrm{GeV}$, corresponds to the effective coupling at the Z boson mass scale $\alpha_s(M_Z^2) = 0.111$. The factorization scale is $\mu_F = 2m_c$, the renormalization one is $\mu_R = m_c$, where the charm quark mass, m_c, is chosen to be equal 1.3. The sea-level prompt muon flux was parameterized by authors (Pasquali et al., 1999) as

$$\log_{10}[E_\mu^3 \phi_\mu^{D,\Lambda_c}(E_\mu)/(\mathrm{cm}^{-2}\mathrm{s}^{-1}\mathrm{sr}^{-1}\mathrm{GeV}^2)] = -5.91 + 0.290y + 0.143y^2 - 0.0147y^3, \quad (1)$$

where $y = \log_{10}(E_\mu/\mathrm{GeV})$.

PRS-2:

In the PRS-2 model (identical with the PQCD-2 in Ref. (Sinegovskaya and Sinegovsky, 2001)), CTEQ3M set (Lai et al., 1995) was used. Corresponding inputs that were utilized in this model are $\Lambda_4^{\overline{MS}} = 0.239$ GeV, $\alpha_s(M_Z^2) = 0.112$, $m_c = 1.3$ GeV, $\mu_F = 2m_c$, $\mu_R = m_c$, and $\lambda = 0.286$ at $Q_0^2 = 1.6\,\mathrm{GeV}$. The corresponding PM flux was parameterized as

$$\log_{10}[E_\mu^3 \phi_\mu^{D,\Lambda_c}(E_\mu)/(\mathrm{cm}^{-2}\mathrm{s}^{-1}\mathrm{sr}^{-1}\mathrm{GeV}^2)] = -5.79 + 0.345y + 0.105y^2 - 0.0127y^3. \quad (2)$$

PRS-3:

In this model the CTEQ3M set was also used. Differing from PRS-2 in renormalization and factorization scales, $\mu_F = \mu_R = m_c$, this model appears the uncertainty due to the scale choice. The PM spectrum predicted is now

$$\log_{10}[E_\mu^3 \phi_\mu^{D,\Lambda_c}(E_\mu)/(\mathrm{cm}^{-2}\mathrm{s}^{-1}\mathrm{sr}^{-1}\mathrm{GeV}^2)] = -5.37 + 0.0191y + 0.156y^2 - 0.0153y^3. \quad (3)$$

GGV:

Here we present results for the model, among those discussed by Gelmini et al. (2001), which is based on MRST set of PDFs (Martin et al., 1999) with different values of the slope λ in the range $0.1-0.5$, $Q^2 \geq 1.25\,\mathrm{GeV}^2$; $\alpha_s(M_Z^2) = 0.1175$. The factorization and renormalization scales are:

$$\mu_F = 2m_T,\ \mu_R = m_T,$$

where

$$m_T = (k_T^2 + m_c^2)^{1/2},\ m_c = 1.25\,\mathrm{GeV},$$

and characteristic transverse momentum k_T is of $\sim m_c$.

In order to compute PM flux underwater we parameterize with Eq. (4) sea-level muon spectra of the GGV model (see Fig. 7 in Ref. (Gelmini et al., 2001)):

$$\phi_\mu^{D,\Lambda_c}(E_\mu)/(\mathrm{cm}^{-2}\mathrm{s}^{-1}\mathrm{sr}^{-1}\mathrm{GeV}^{-1}) = A\,(E_\mu/\mathrm{GeV})^{-(\gamma_0+\gamma_1 y+\gamma_2 y^2+\gamma_3 y^3)}\,. \quad (4)$$

In Table 1 five sets of the parameters to Eq. (4) are presented

Table 1. λ dependent parameters of the prompt muon differential spectra at the sea level (Eq. (4)).

λ	$A, 10^{-6}$	γ_0	γ_1	$\gamma_2, 10^{-2}$	$\gamma_3, 10^{-3}$
0.1	3.12	2.70	−0.095	1.49	−0.2148
0.2	3.54	2.71	−0.082	1.12	−0.0285
0.3	1.80	2.38	0.045	−0.82	0.911
0.4	0.97	2.09	0.160	−2.57	1.749
0.5	0.58	1.84	0.257	−4.05	2.455

for different values of the small-x gluon PDF spectral index λ.

We calculated the conventional muon flux basing on the nuclear cascade model by Vall et al. (1986) (see also Naumov et al. (1998); Bugaev et al. (1998)). High-energy part of this

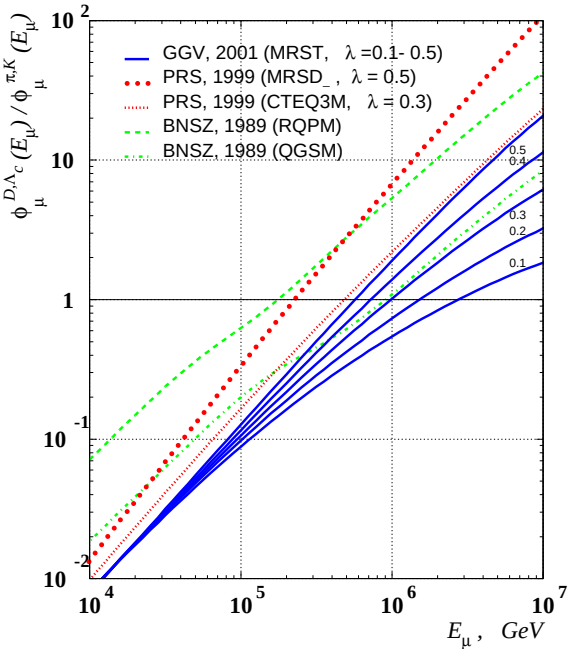

Fig. 2. Sea-level ratio of the differential prompt muon flux to the conventional one.

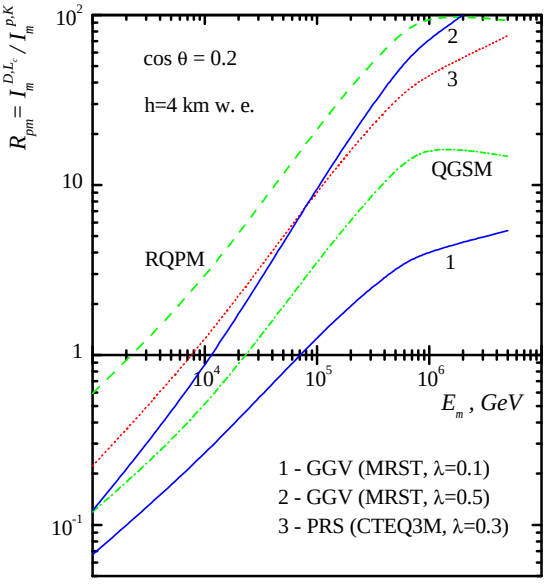

Fig. 3. Prompt muon contribution at $h = 4$ km w. e. vs. E_μ.

spectrum for the vertical may be approximated with formula (in $\mathrm{cm}^{-2}\mathrm{s}^{-1}\mathrm{sr}^{-1}\mathrm{GeV}^{-1}$)

$$\phi_\mu^{\pi,K}(E_\mu, 0^\circ) = \begin{cases} 14.35\, E_\mu^{-3.672} & E_1 < E_\mu \leqslant E_2, \\ 10^3 E_\mu^{-4} & E_\mu > E_2, \end{cases} \quad (5)$$

where $E_1 = 1.5878 \times 10^3$ GeV, $E_2 = 4.1625 \times 10^5$ GeV.

Five thin lines in Fig. 1 present the sum of the conventional muon flux Eq. (5) and the GGV PM flux (Eq. (4)) corresponding to $\lambda = 0.1, 0.2, 0.3, 0.4, 0.5$ (numbers near lines). Dot lines show the same for PRS models, Eqs. (1-3). For comparison there are also shown contributions due to the quark-gluon string model (QGSM) and the recombination quark-parton one (RQPM) (Bugaev et al., 1989, 1998) (dash-dot and dash, respectively). Ratios of PM fluxes according above models to the conventional flux are shown in Fig. 2. As one can see, the cross energy of the PM fluxes and conventional one covers the wide region from $\sim$ 150 TeV to $\sim$ 3 PeV, that is more than one order of the magnitude.

3 Prompt muon component of the flux underwater

Muon energy spectra and angle distributions of the flux underwater was computed with the method by Naumov et al. (1994). The collision integral in the kinetic equation includes the energy loss of muons due to bremsstrahlung, direct e^+e^- pair production and photonuclear interactions. The ionization energy loss and the small-v part of the loss due to e^+e^- pair production ($v < 2 \cdot 10^{-4}$, where v is the fraction of the energy lost by the muon) were treated as continuous ones. In our calculations of underwater muon fluxes at different zenith angles, we used PQCD PM fluxes calculated only for the vertical direction, supposing the isotropic approximation for prompt muons to be a reliable at least for $10^4 < E_\mu < 10^6$ GeV at zenith angles $\theta \lesssim 80^\circ$.

The prompt muon fraction of the flux underwater, R_{pm}, defined as ratio of the integral prompt muon spectrum to the conventional one, is presented in Fig. 3 for the depth of 4 km of the water equivalent (w. e.) and for $\cos\theta = 0.2$. As is seen from the figure, R_{pm} related to the gluon density slope $\lambda = 0.5$ is a factor 3 greater than that for $\lambda = 0.1$ at $E_\mu \gtrsim 10$ TeV.

Zenith-angle distributions of the prompt muon contribution at depths $1 - 4$ km w. e., calculated for $E_\mu > 100$ TeV, are shown in Fig. 4. Only GGV model predictions were used here with $\lambda = 0.1$ (dash) and $\lambda = 0.5$ (solid). For the vertical one can see R_{pm} rising from about 0.2 at the depth of Baikal NT (1.15 km) to about 0.5 at the NESTOR depth (~ 4 km). For the larger zenith angles, $\theta \sim 75^\circ$, this contribution becomes apparently sizable at depths $3 - 4$ km. Differences in the predictions owing to a change of λ, from 0.1 to 0.5 (see $h = 2$ and 3 km w. e.), are also clearly visible: the ratio $R_{pm}(\lambda = 0.5)/R_{pm}(\lambda = 0.1)$ at $h = 2$ km w. e. grows from about 1.5 to about 5 as $\cos\theta$ changes from 1 to 0.2.

Here we supposed no differences between the PRS and GGV models apart from those related to the charm production cross sections. Actually one needs to compare the primary spectrum and composition, nucleon and meson production cross sections and other details of the atmospheric nuclear cascade being used in above computations. These sources of uncertainties would be considered elsewhere.

4 Summary

In order to test the small-x gluon distribution effect we have computed deep-sea prompt muon fluxes using predictions of

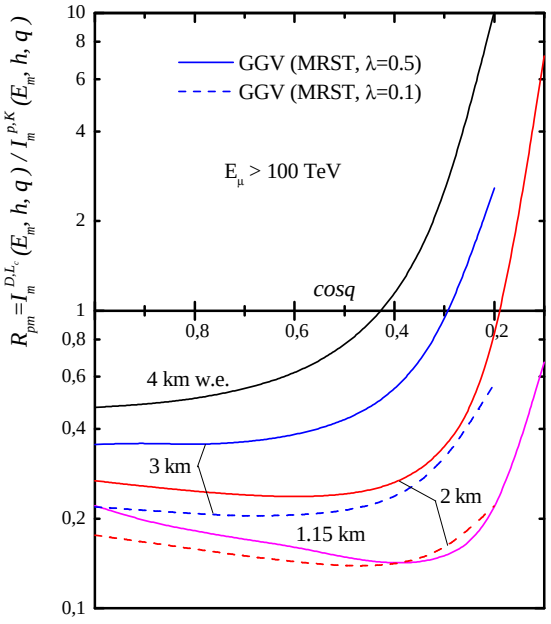

Fig. 4. Ratio of the prompt muon flux underwater to the conventional one as a function of $\cos\theta$.

charm production models based on NLO calculations of the PQCD (Pasquali et al., 1999; Gelmini et al., 2001). The possibility to discriminate the PQCD models, differing in the slope of the gluon distribution, seems to be achievable in measurements of the underwater muon flux at energies 10-100 TeV.

Being hardly appeared at the sea level for energies up to 10^5 GeV (Figs. 1, 2), a dependence on the spectral index λ of the small-x gluon distribution becomes more distinct at depths $3-4$ km w. e. (Figs. 3, 4). At the depth of 4 km and at the angle of $\sim 78^\circ$ one could observe the PM flux to be equal, for $\lambda = 0.5$, to the conventional one even for muon energy ~ 10 TeV (the cross energy). While for $\lambda = 0.1$ the cross energy is about 70 TeV. For the high energy threshold, $E_\mu > 100$ TeV, and at $h \lesssim 3$ km w. e., the ratio R_{pm} is nearly isotropic up to $\sim 60^\circ$. The "cross zenith angle" at a given depth, $\theta_c(h)$, depends apparently on λ:

$$\cos\theta_c\,|_{\lambda=0.5} \simeq 0.3,\ \cos\theta_c\,|_{\lambda=0.1} \simeq 0.1,\ h = 3\ \mathrm{km\,w.e.}$$

Acknowledgements. The work of T. S. and S. S. is supported in part by the Ministry of Education of the Russian Federation under Grant No. 015.02.01.004 (the Program "Universities of Russia – Basic Research").

References

Amram, P., et al. (ANTARES Collaboration), Background light in potential sites for the ANTARES undersea neutrino telescope, Astropart. Phys., **13**, 127–136, 2000.

Anassontzis, E. G., et al. (NESTOR Collaboration), NESTOR: a status report, Nucl. Phys. B (Proc. Suppl.), **85**, 153-156, 2000.

Andres, E., et al. (AMANDA Collaboration), The AMANDA neutrino telescope: principle of operation and first results, Astropart. Phys., **13**, 1–20, 2000.

Balitsky, Ya. Ya. and Lipatov, L. N., The Pomeranchuk singularity in quantum chromodynamics, Sov. J. Nucl. Phys., **28**, 822–829, 1978; Kuraev, E. A., Lipatov, L. N., and Fadin, V. S., The Pomeranchuk singularity in non-Abelian gauge theories, Sov. Phys. JETP, **45**, 199–204, 1977.

Ball, R. D. and Landshoff, P. V., The challenge of small x, J. Phys. G: Nucl. Part. Phys., **26**, 672-682, 2000.

Belolaptikov, I. A., et al. (Baikal Collaboration), The Baikal underwater neutrino telescope: Design, performance, and first results, Astropart. Phys., **7**, 263–282, 1997.

Bugaev, E. V., et al., Prompt leptons in cosmic rays, Nuovo Cim., C **12**, 41–73, 1989.

Bugaev, E. V., et al. Atmospheric muon flux at sea level, underground, and underwater, Phys. Rev., D **58**, 054001, 1–27, 1998.

Gelmini, G., Gondolo, P., and Varieschi, G., Prompt atmospheric neutrinos and muons: Dependence on the gluon distribution function, Phys. Rev., D **61**, 056011, 1–12, 2000.

Gelmini, G., Gondolo, P., and Varieschi, G., Measurement of the gluon parton distribution function at small x with neutrino telescopes, Phys. Rev., D **63**, 036006, 1–14, 2001.

Lai, H. L., et al., Global QCD analysis and the CTEQ parton distributions, Phys. Rev., D **51**, 4763–4782, 1995; Lai, H. L., et al., Improved parton distributions from global analysis of recent deep inelastic scattering and inclusive jet data, Phys. Rev., D **55**, 1280–1296, 1997.

Lai, H. L., et al., Global QCD analyses of parton structure of the nucleon: CTEQ5 parton distributions, Eur. Phys. J., C **12**, 375–392, 2000.

Learned, J. G. and Mannheim, K., High-energy neutrino astrophysics, Ann. Rev. Nucl. Part. Sci., **50**, 679–749 , 2000.

Martin, A. D., Stirling, W. J., and Roberts, R. G., New information on parton distributions, Phys. Rev., D **47**, 867–882, 1993.

Martin, A. D., Roberts, R. G., Stirling, W. J., and Torne, R. S., Update of MRST partons, Nucl. Phys. B (Proc. Suppl.), **79**, 105-107, 1999; hep-ph/9906231, 3 p.

Naumov, V. A., Sinegovskaya, T. S., and Sinegovsky, S. I., Potential of deep–underwater neutrino telescopes for recording muons from charm decay, Yad. Fiz., **63**, 2016–2019, 2000 [Phys. Atom. Nucl. **63**, 1923–1926, 2000].

Naumov, V. A., Sinegovskaya, T. S., and Sinegovsky, S. I., $K_{\ell 3}$ form factors and atmospheric neutrino flavor ratio at high energies, Nuovo Cim., A **111**, 129–148, 1998.

Naumov, V. A., Sinegovsky, S. I., and Bugaev, E. V., A new method for calculating the energy spectrum of cosmic ray muons under thick layers of matter, Yad. Fiz. **57**, 439–451, 1994 [Phys. Atom. Nucl. **57**, 412–424, 1994].

Pasquali, L., Reno, M. H., and Sarcevic, I., Lepton fluxes from atmospheric charm, Phys. Rev., D **59**, 034020, 1–10, 1999.

Schleper, P., Soft hadronic interactions, hep-ex/0102051, 14p.

Sinegovskaya, T. S. and Sinegovsky, S. I., Prompt muon contribution to the flux underwater, Phys. Rev., D **63**, 096004, 1–6, 2001.

Vall, A. N., Naumov, V. A., and Sinegovsky, S. I., The hadronic component of high-energy cosmic rays and the growth of the inelastic cross sections, Yad. Fiz., **44**, 1240–1250, 1986 [Sov. J. Nucl. Phys. **44**, 806–812, 1986].

Vogt, R., Physics of the nucleon sea quark distributions, Prog. Part. Nucl. Phys., **45**, S105-S169, 2000 [hep-ph/0011298].

Yoshida, R. (on behalf of ZEUS and H1 Collaboration), HERA small-x and/or diffraction, hep-ph/0102262, 20 p.